

Impact of Mixed Solvent on Co-Crystal Solubility, Ternary Phase Diagram, and Crystallization Scale Up

Tasnim Munshi,^{*,†} Batul Redha,[†] Neil Feeder,[‡] Paul Meenan,[§] and Nicholas Blagden^{||}

[†]School of Chemistry, University of Lincoln, Lincoln, U.K. LN6 7TS

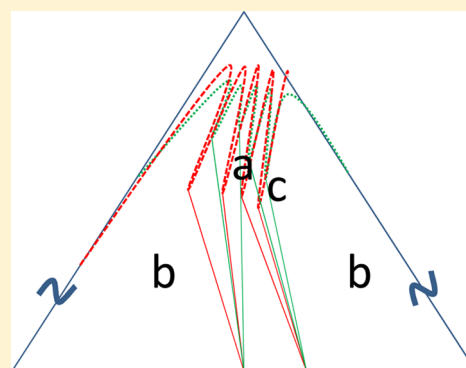
[‡]Cambridge Crystallographic Data Centre, 12 Union Road, Cambridge, U.K.

[§]Pfizer Global Research & Development, Pharmaceutical Sciences, Sandwich, U.K. and Pharmaceutical Sciences, Pfizer Global R & D, Groton, Connecticut 06340, United States

^{||}School of Pharmacy, University of Lincoln, Lincoln, U.K. LN6 7TS

S Supporting Information

ABSTRACT: This contribution covers the identification, understanding, and rationale of the interplay between the choice of mixed solvent on the crystallization of the co-crystal system benzoic acid and isonicotinamide (BZ:INA). A critical first step was gauging the impact of solvent choice and composition on the overall crystallization process, across a number of temperature points. This required defining the solubility and phase diagrams of the co-crystal system at specified temperatures, which reflects the cooling crystallization profile encountered in a batch crystallization step. To this end, identifying and understanding the impact of solvent composition over a selected temperature range on the solubility of co-crystal underpins this contribution.



INTRODUCTION

Significant literature exists on the design and synthesis of co-crystals and the application of co-crystals in drug development.¹ However, the focus of this contribution centers on the area of bulk crystallization and the scale up of the solution crystallization route. This aspect of co-crystal research is presently an unexplored area, but critical insight is required if co-crystals are to be routinely isolated from solution and used in the fine chemical and pharmaceutical sectors.

The motivation for considering the application of co-crystals as a dosage form stems from the need to generate stable crystalline material in order to have selectivity and control over the chemical and physical properties of drug entities,¹ specifically, increasing the solubility and manipulating the dissolution profile in order to improve bioavailability. Allied to this is the notion that the solubility of the drug is related to drug absorption, and in the crystallization process there is a need to have knowledge of the solubility profiles and many studies had been carried out and reported.² These have focused on the trends of polymorph solubility, dissolution and thermodynamic behavior, and the impact of thermodynamic and kinetic factors on the formation of different polymorphs.³ This study is the natural progression of these types of concepts for polymorphic systems to co-crystal systems.

The purpose of this work is to examine the role of solvent and a mixed solvent composition on the solution co-crystallisation process. We have chosen the isonicotinamide (INA) and benzoic acid (BA) co-crystal system, as much

literature exists in the determination of co-crystal growth from these two compounds in a single solvent and the impact of component ratio through complex formation of the 1:1 and 2:1 complexes.^{4,5} It has been previously reported how differences in solubility of the compounds map onto the profile of a typical ternary phase diagram for a 1:1 co-crystal, with compounds with different solubility mapping to the formation of a skewed phase diagram.⁶ We report here a more complex situation where a co-crystal has both a 1:1 and 2:1 complex, when a mixed system is employed, and will examine the impact of this in designing the co-crystallisation isolation step.

We report specifically on the impact of a (i) mixed solvent through manipulating the solubility of cofomers and molecular complexes and (ii) the impact of composition on the compounds as defined by the ternary phase diagram and how these contribute to the design of the crystallization for this class of compounds.

The solubility of co-crystals in a 1:1 and 2:1 composition in the mixed solvents was analyzed and determined by a single mathematical equation, and data were fitted to the cosolvency model of the general single model (GSM).⁷ In order to determine the thermodynamic factors that control the formation of these molecular systems, the change in enthalpy

Received: June 30, 2015

Revised: February 17, 2016

71 and entropy in solution was determined using the van't Hoff
72 equation.

73 ■ MATERIALS AND METHODS

74 For further details on the experimental details, see [Supporting](#)
75 [Information](#) and the Redhas thesis.⁸

76 All chemicals were purchased from Sigma-Aldrich in the highest
77 purity and were used as supplied.

78 Co-crystals were grown in water, ethanol, and an ethanol/water
79 solvent (30–90% ethanol). The products were characterized by
80 powder X-ray diffraction (PXRD), Raman, infrared, and ¹H NMR
81 spectroscopy.

82 **Solubility.** The Jouyban–Acree model was used to predict the
83 solubility of co-crystal,^{8–11} and the solubility was also determined
84 experimentally (see [Supporting Information](#)).

85 **X-ray Powder Diffraction.** Samples were analyzed using a Bruker
86 D8 diffractometer (wavelength of X-ray 0.154 nm Cu source). The
87 solids were scanned from 5–50°, with a 0.01 step width and 1 s time
88 count. The receiving slit was 1°, and the scatter slit was 0.2°.

89 **Solubility Determination.** The React-Array Microvate (low
90 throughput) was used to determine the solubility. The samples were
91 placed in glass tubes, and the solutions were stirred at temperatures of
92 25, 35, and 40 °C, the samples were held at these temperatures for 80
93 h, and then the solubility was determined gravimetrically.

94 The predicted solubility in the mixed solvent was calculated using
95 the Jouyban–Acree model, and the deviation from the experimental
96 solubility was determined.^{12,13}

97 **Phase Diagram.** The screen method developed by Blagden and
98 Boyd et al. was used for this study.^{5,14} The RUMED incubator was
99 used to incubate the slurry solution for 2 weeks, and the phases were
100 determined with PXRD.

101 The ternary phase diagram was constructed at 20 and 40 °C, in 50%
102 ethanol, and the solids were analyzed using PXRD. These ternary
103 phase diagram was plotted using the ProSim software ternary diagram
104 plot.¹⁶

105 The phase diagrams, along with the solubility at 50% ethanol
106 solution composition, were subsequently employed to design the
107 cooling crystallization at 100 cm³ volume.

108 ■ RESULTS AND DISCUSSION

109 **Solubility.** First, the solubility of benzoic acid, isonicotina-
110 mide, and 1:1 and 2:1 co-crystals at 25 and 40 °C was
111 determined in water, ethanol, and a water/ethanol mixed
112 solvent (30–90% ethanol), and the change in the solubility was
113 observed. Second, for completeness the direct solubility of the
114 co-crystals and cofomers in a mixed solvent was also analyzed,
115 and a hyperbolic solubility profile was observed; the values in
116 pure solvent agree with those previously reported.⁵

117 In order to undertake the van't Hoff equation, an analysis of
118 the solubility curves of the co-crystal was redrawn such that ln
119 solubility vs 1/temp was plotted, and the profiles for solubility
120 are given in [Figure 1a](#) and [Figure 1b](#) for the 1:1 and 2:1 co-
121 crystals, respectively (see [Supporting Information](#)).

122 **Solubility Behavior of Co-Crystal Cofomers in a**
123 **Mixed Solvent System.** The solubility behavior of the 1:1
124 and 2:1 co-crystals was examined as the water to ethanol
125 content was varied. For both co-crystals, the solubility was at a
126 minimum in water and increased as the solvent composition
127 approached 70% v/v and decreased as the ethanol composition
128 increased. The trend was highly distinctive for the 2:1 co-crystal
129 system ([Figure 2](#)).

130 The trends in molar enthalpy and entropy for both the 1:1
131 and 2:1 co-crystal systems ([Figure 2](#)) are similar for both
132 systems, and the enthalpy is consistent and does not change as
133 the ethanol concentration is increased; however, a notable
134 variation is seen as the concentration of ethanol is increased.

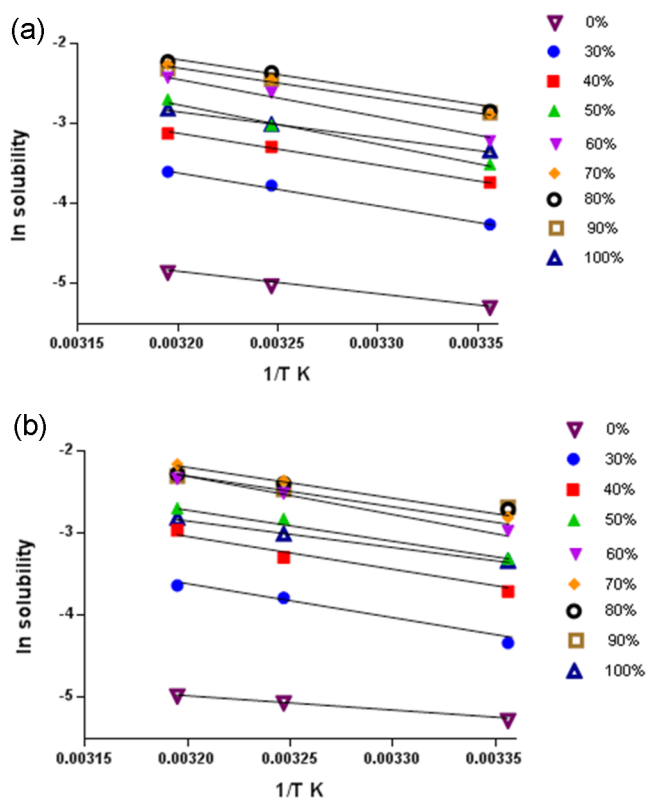


Figure 1. (a) Change in the solubility of co-crystal (1:1) with the inverse of the change of temperature. (b) Change in the solubility of co-crystal (2:1) with the inverse of the change of temperature.

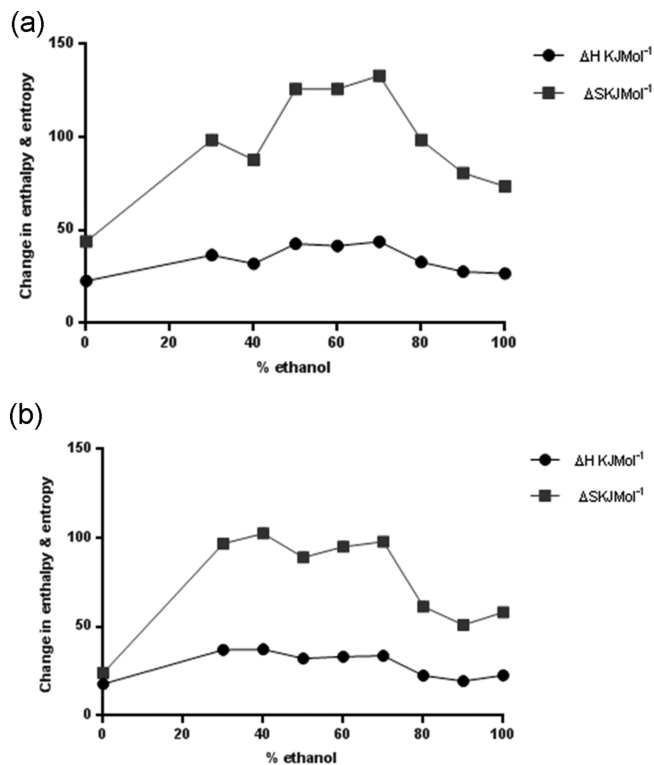


Figure 2. (a) Change in ΔH molar enthalpy of solution, ΔS molar entropy of solution of co-crystals 1:1 in solution. (b) Change in ΔH the molar enthalpy of solution, ΔS the molar entropy of solution of co-crystals 2:1 in solution.

The implication of these profiles is that the mode of assembly (e.g., hydrogen bond usage and solute solvent interaction) is consistent between the levels of association, i.e., monomers, dimers, chains, etc.; however, the level of assembly varies with regard to the solvation cage and molecular association. This inference is consistent, with a similar mode assembly between the 1:1 and 1:2 occurring in the solution, mirroring the mode of assembly in the crystal structures, in that the enthalpy has a similar but less marked behavior to entropy.

Another approach to the solubility trends is to model solubility in a mixed solvent. A current model used to determine solubility in mixed solvents is the Jouyban–Acree model.⁷ A generic model based on the Jouyban–Acree model was developed by training using the literature data for an ethanol/water mixed solvent (see Supporting Information). The model gives poor results for this system because of the two cofomers, which overcomplicates the system.

Summary of Solubility Trends. The deviation of the actual solubility from the ideal solubility may indicate that there is a solute–solvent interaction. This suggests that it is critical to obtain verification of nonideal contribution, which may be achieved by examining the deviation from idealities of the measured solubility's (W) to those of the calculated ideal (Q) at a specific temperature (deviation taken as W/QT = solubility in mixed solvent/log–linear model at specific temperatures, see Supporting Information).

For this reason the deviation in actual solubility from the ideal solubility obtained by the ratio of experimental solubility with the ideal solubility calculated using solvent fraction and solute cofomer solubility in the respective pure solvents was examined at 25 °C (blue), 35 °C (red), and 40 °C (green) Figure 3a (1:1) and Figure 3b (2:1).

This approach clearly verifies the observations seen with the solubility fitting, whereby two distinct variable solutions

regimes exist, and these are dependent on temperature, irrespective of the stoichiometric ratio. This type of trend also suggests that the water breaks up the association and thus affects the balance of monomers versus dimers, etc., as does increasing the temperature, and this is supported by the profiles obtained as the amount of water is increased (Figure 3).

Optimising the Solution Crystallization Conditions. The phase diagrams and subsequent crystallization studies focused on the 40 to 20 °C temperature range, and these were undertaken in an ethanol–water composition determined by the solubility studies; all solutions prior to crystallization were saturated at 40 °C and taken to 50 °C to ensure complete dissolution. The clearest way to extract the initial solvent composition point was to examine the solubility profiles and to confirm the % composition point, for this work 50% was identified. This was undertaken in order to maximize the hypothetical yield, which for our purposes was the highest possible amount of material in solution, and typically this was around 45–55%. From this starting point, two linked studies were undertaken, (i) slow cooling from 50 °C at a rate of 1 to 0.5 °C, to determine the point at which crystallization occurs; this is taken as the under cooling point for our purposes, Figures 4a and 5a, and (ii) step cooling crystallizations from 50 °C to the identified under cooling point, to determine the time for crystallization to occur; which relates to the induction time, Figures 4b and 5b. This is taken as the induction time for crystallization for our purposes.

For the 1:1 system, the curve profile shows that the temperature was at its lowest when the co-crystals were grown

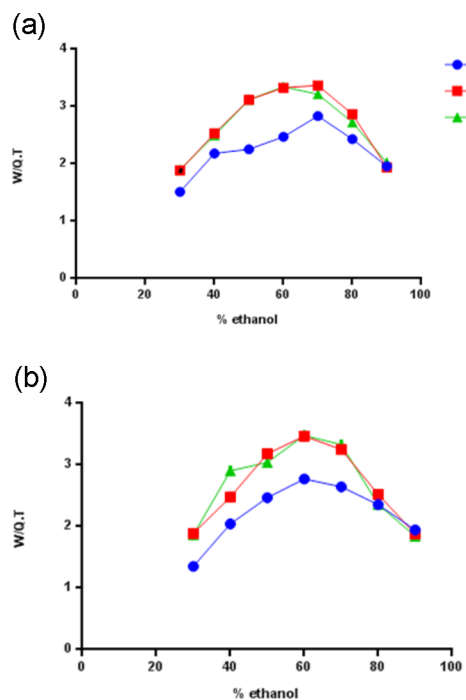


Figure 3. (a) Deviation of the solubility of co-crystals (1:1) in the mixed solvent from ideal solubility. (b) Deviation of the solubility of co-crystals (2:1) in the mixed solvent from ideal solubility.

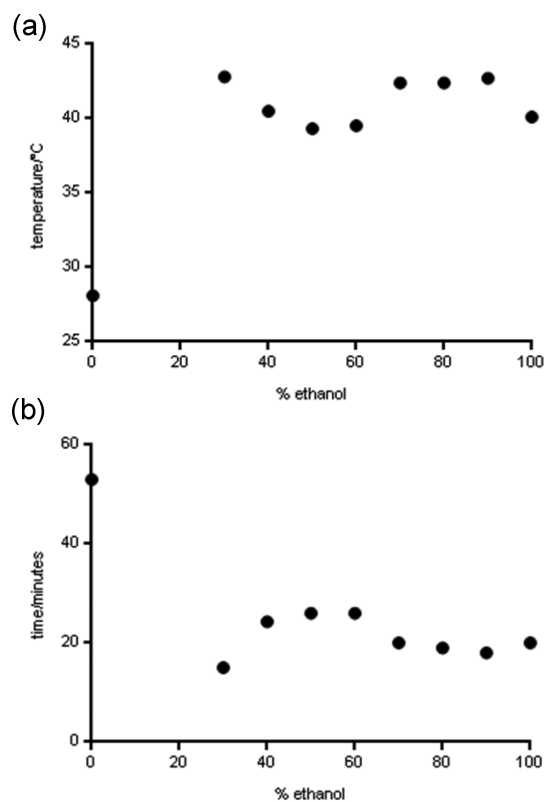


Figure 4. (a) Onset crystallization temperature, relates to the undercooling from 50 °C, BZ:INA (1:1) in water, ethanol, and ethanol/water mixture. (b) Induction time required to start crystallization from the undercooling point from BZ:INA (1:1) in water, ethanol, and ethanol/water mixture.

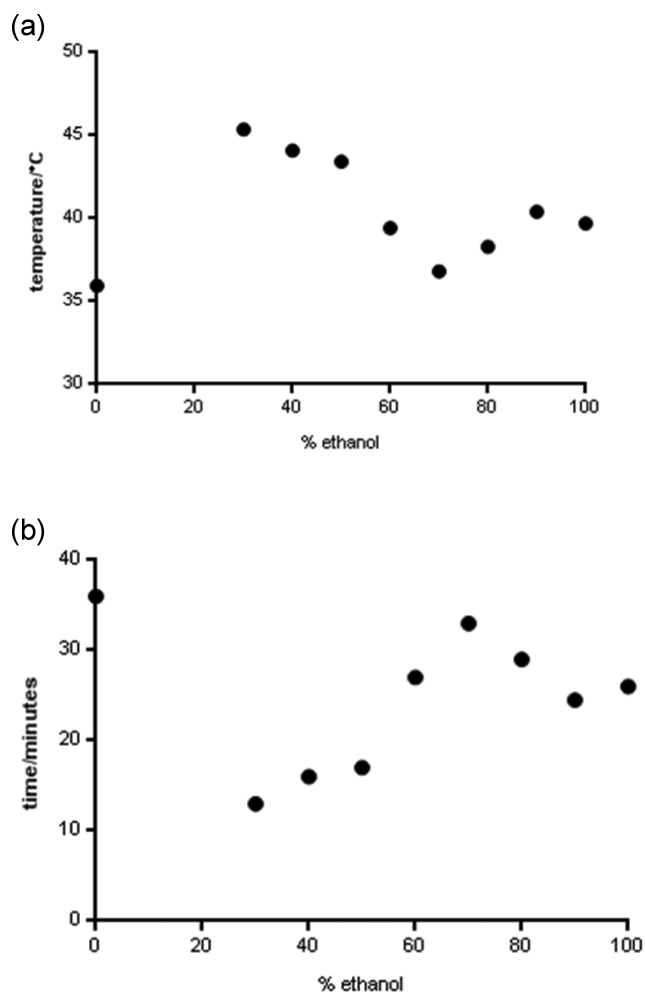


Figure 5. (a) Onset crystallization temperature relates to the undercooling from 50 °C of BZ:INA (2:1) in water, ethanol, and ethanol–water mixture. (b) Induction time required to start crystallization from the undercooling point from of BZ:INA (2:1) in water, ethanol, and ethanol–water mixture.

198 in water at 28 °C, as the concentration of ethanol was increased
 199 the temperature increased sharply in the 30% ethanol solvent
 200 and reached 42.8 °C, while the temperature fluctuated between
 201 39.3–42.8 °C at higher ethanol concentration. The maximum
 202 time for the start of crystallization in water was 53 min (Figure
 203 4), and the time in 30% ethanol–water mixture was 15 min.
 204 The time for the onset of crystallization was found to have
 205 increased to 26 min at 50–60% ethanol, and it fluctuated as the
 206 concentration of ethanol was increased.

207 For the 2:1 system the curve profile shows that the
 208 crystallization onset temperature in water was low (36 °C),
 209 and the temperature increased to 45.4 °C in 30% ethanol, and
 210 the temperature dropped to 36 °C in the 70% ethanol solvent
 211 and fluctuated as the concentration of ethanol was increased.
 212 The curve profile for the induction time for the 2:1 co-crystal
 213 indicates that the maximum time required for the start of
 214 crystallization in water was 39 min, the time dropped sharply to
 215 15 min in the 30% ethanol mixture, and the time of
 216 crystallization increased to 30 min at 50–60% ethanol
 217 concentration and decreased further as the concentration of
 218 ethanol was increased to around 22 min.

219 These overall sets of undercooling and induction time data
 220 indicate that in pure water the crystallization process would

221 proceed more rapidly than at other solution compositions, and
 222 with less under cooling. In addition, the 1:1 system at greater
 223 than 50% ethanol appears to behave consistently, whereas the
 224 2:1 system over a similar composition range appears to go
 225 through a maximum and then decrease over the same
 226 composition range. This may be a facet of a kinetic of the
 227 crystallization process of this system, and therefore the phase
 228 diagram for this system was re-evaluated at 20 °C and also at 40
 229 °C. These two phase diagrams were then taken as the
 230 thermodynamic start and end point of the step cooling
 231 crystallization process.

The Ternary Phase Diagram at 20 and 40 °C. The phase
 232 diagram at 20 and 40 °C shows a skewed profile at both
 233 temperatures, which reflects the differences in the solubility in
 234 50% ethanol of benzoic acid and isonicotinamide. Similar work
 235 carried out by Seaton et al.⁵ in pure solvents at 25 °C showed
 236 that the phase diagram in the water system was heavily skewed,
 237 but both 1:1 and 1:2 phases can be grown, while in the ethanol
 238 system only co-crystals 1:1 were grown and was less skewed.
 239

The solubility within the phase diagrams at the two
 240 temperatures defines the start and end point for a temperature
 241 drop cooling crystallization. To link the two isothermal points
 242 of the phase diagrams with thermodynamic phase equilibrium
 243 points during the step crystallization process, it is important to
 244 recognize the deviation in the solubility line between the two
 245 temperatures, in defining the labile region during the step
 246 cooling process which drives supersaturation. This schematic
 247 was derived from overlaying the two phase diagram with the
 248 scaling focused upon the eutectic/solubility regions over the
 249 region which defines 1:1 only, 1:1 concurrent with 2:1 and 2:1
 250 only. Figure 6 highlights the viable labile region for the
 251 1:1

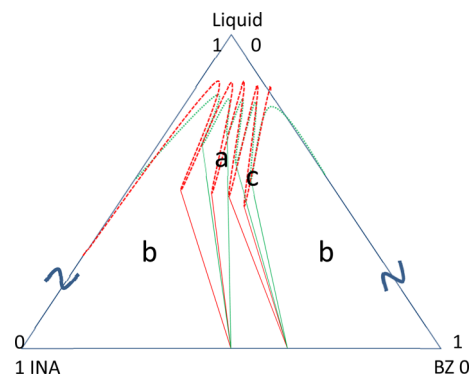


Figure 6. This schematic highlights the deviation between the ternary phase diagrams at 20 °C (dash lines) and 40 °C (solid line). (a) For 1:1, (b) concurrent region, and (c) for 2:1.

crystallization from 40 °C (solid) to 20 °C (dash) for specific
 252 solid phase compositions, marked (a) for 1:1, (b) concurrent
 253 region, and (c) for 2:1 respectively.
 254

This approach was taken to specify the crystallization
 255 conditions in which the system was driven through the labile
 256 region at 50 °C, through the phase equilibrium at 40 °C and
 257 onto phase equilibrium at 20 °C; these two latter temperature
 258 points define the thermal separation employed for these
 259 studies. Selection was based upon creating a cooling profile
 260 with composition which would establish conditions for
 261 crystallization in which one co-crystal phase relation to another
 262 could be examined.¹⁶ With regard to the phase diagrams, 263
 264 cooling a solution below its *liquidus* line at tie line requires
 265 refined screening to define the transition from one crystal

266 composition to another in order to define the tie line
267 boundary¹⁷ and defines the regions on concurrent phase
268 formation. Thus, it is important to use the full set of
269 constructed ternary phase diagrams at various solution
270 compositions to identify the optimum cooling crystallization.

271 **Solution Crystallization – 1:1 to 2:1 Interconversions
272 and Role of Seeding.** The details of deviation in the
273 solubility, tie lines, size, and position of the different regions
274 and the eutectic points are presented in Figures 7 and 8. The

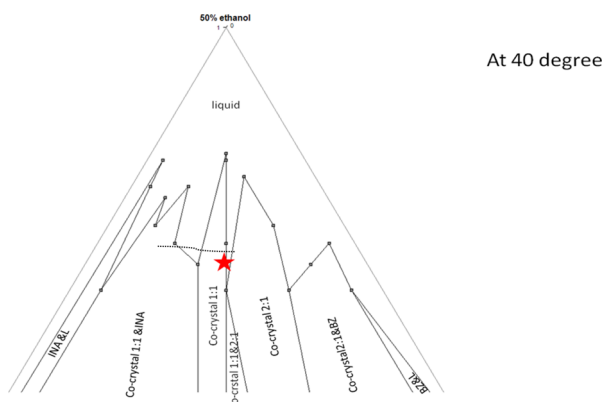


Figure 7. Upper part of the ternary phase diagram of benzoic acid, isonicotinamide, and 50% ethanol at 40 °C (the red point shows the composition of the mixture used in this experiment).

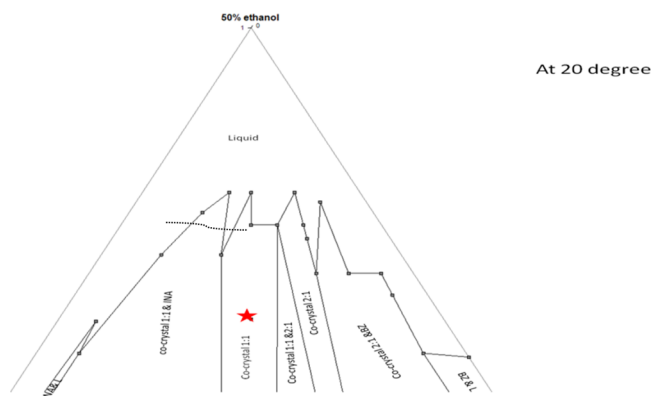


Figure 8. Upper part of the ternary phase diagram of benzoic acid, isonicotinamide, and 50% ethanol at 20 °C (the red point shows the same composition of the mixture used at 20 °C in this experiment).

275 red star on the liquid solid line identifies where starting at 40
276 °C would relate to 20 °C for 1:1 co-crystal, e.g., as defined by
277 the detail of the component solubility and eutectics. Gradual
278 cooling shows the formation of co-crystals 2:1 from BZ:INA
279 (1:1) in 50% ethanol, and cooling indicates that the 2:1 product
280 is kinetically favored over the 1:1 co-crystal.

281 This was confirmed by examining the powder X-ray
282 diffraction pattern of the solid formed during crystallization
283 with and without seeding. These studies indicate that co-
284 crystals 2:1 were grown when the crystals were left to grow for
285 1 h, the formation of co-crystals 2:1 were kinetically favored,
286 and there was no effect of 1:1 seeds to enhance the growth of
287 co-crystal 1:1 instead of 2:1, but when the crystals were left to
288 grow over a longer period, only formation of the 1:1 co-crystals
289 occurred. This indicates the 1:1 co-crystals were thermody-
290 namically favored. It is for this reason that the isothermal
291 ternary phase diagrams have been redrawn to indicate *meta*

292 stability (Figures 7 and 8), as indicated by the dash line in the
293 upper most portions of the phase regions for 1:1 only,
294 concurrent 1:1 with 2:1 and 2:1 only. The drawn out cooling
295 crystallization in 50% ethanol shows the formation of co-
296 crystals 2:1 from BZ:INA (1:1) in 50% ethanol, and this
297 indicates that this product is kinetically favored over the 1:1
298 system.

299 Starting with the physical mixture of BZ:INA (1:1) the
300 monitoring of crystallization confirms the previous report that
301 only 2:1 co-crystals were grown in water and only 1:1 co-
302 crystals were grown in ethanol.⁵ When the physical mixture of
303 BZ:INA was set at a 2:1 stoichiometric ratio, and the solvent
304 composition was varied, the crystal screening clearly showed
305 that an increase in the formation of 2:1 co-crystals was noted as
306 the fraction of water increased, and an increase in 1:1 co-
307 crystals was noted as the fraction of ethanol was increased. This
308 leads to the possibility of tuning the crystallization outcome
309 through the selection of an appropriate solvent composition.

310 To highlight this tuneability opportunity for the crystal-
311 lization on solvent composition, the phase outcome was
312 monitored, and the solution composition was varied from pure
313 water to pure ethanol for a batch cooling crystallization run.
314 Typical outcomes are presented in Figures 9 and 10. As the

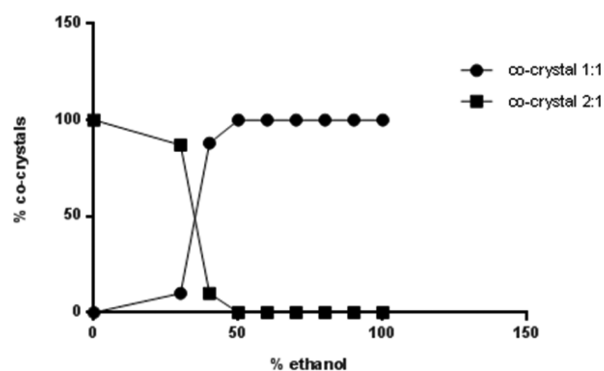


Figure 9. Change in the growth of co-crystals (1:1) and (2:1) from BZ:INA (1:1) with the change of the solvent.

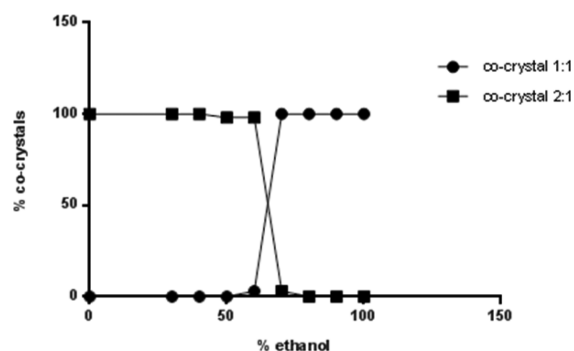


Figure 10. Change in the growth of co-crystals (1:1) and (2:1) from BZ:INA (2:1) with the change of the solvent.

315 solvent mixture being varied with either a 1:1 or 2:1 compound
316 ratio being set, the dominate phase around 30% and 40%
317 respectively for the ethanol mixed solvent was the 2:1 system,
318 and for 60 to 100% the dominant phase was 1:1 only.

319 Initially the amount of BZ:INA 1:1 clearly varied as the
320 solvent composition was varied (Figure 9). The curve profile
321 shows that only co-crystals 2:1 were grown in water and only
322 co-crystals 1:1 were grown in ethanol. The growth of 1:1 co-

323 crystals started in 30% ethanol and increased as the growth of
324 2:1 co-crystals decreased with an increase in the concentration
325 of ethanol; however at 60% only 1:1 co-crystals formed.

326 The curve profile (Figure 10) shows that in water only 2:1
327 co-crystals were grown and only 1:1 in ethanol. At 50% ethanol
328 there was significant growth of the 1:1 co-crystals, and with an
329 increase in concentration of ethanol this increased and the
330 amount of 2:1 co-crystals decreased. In 100% ethanol only 1:1
331 cocrytals were grown and at 60% both 1:1 and 2:1 were most
332 significant.

333 With the seeding studies undertaken, to disrupt inter
334 conversion, the following comparative trends without and
335 with seeding were noted. With the crystallization configured for
336 1:1 formation, this phase was observed after 1 h. However,
337 repeating with seeds of 1:1 co-crystals the initial appearance of
338 2:1 as a transient phase was reduced, and conversion to
339 complete 1:1 co-crystals was within 5–10 min. With the
340 crystallization configured for 2:1 formation, this phase was
341 observed after 1 h, and there was no effect of 1:1 seeds to
342 enhance the growth of the 1:1 co-crystal, over the 2:1 within
343 this period.

344 ■ CONCLUSION

345 The solubility of both 1:1 and 2:1 co-crystals increased, with an
346 increase in concentration of ethanol and with an increase in
347 temperature. The solubility of the 2:1 co-crystal is greater than
348 the 1:1 co-crystal in the ethanol–water mixtures, in water the
349 solubility is identical, and at higher ethanol concentration the
350 solubility is similar. Overall, the solubility of 1:1 and 2:1 co-
351 crystals was lower than the solubility of the individual
352 components.

353 Further, this study indicates that the solubility of the 1:1 and
354 2:1 co-crystals in the mixed solvents was fitted to the general AJ
355 model cosolvency, and the overall fit was within an MPD of
356 20%; the model does not really work for this class of
357 compounds. Subsequently, fitting to these studies specific
358 data a MPD of less than 10% was achieved. In fact, two classes
359 of solubility appear to be present, and which grouping they
360 belong to was found to be dependent on temperature and
361 solvent composition. This was further highlighted by examining
362 the deviation of the actual solubility from the ideal solubility.
363 Such deviation suggests that there is reconfiguration in solute–
364 solvent interaction during formation of molecular aggregates or
365 the formation of specific modes of molecular complexation, as
366 seen in the solid state. The van't Hoff equation was used to
367 calculate the enthalpy and entropy of solution; the results show
368 that the enthalpy of solution change for the 1:1 co-crystals is
369 higher than that of the 2:1 co-crystals, indicating that the 1:1
370 co-crystal has more interaction between the solute and the
371 solvent. The entropy of solution change in 1:1 co-crystal is
372 higher than that for 2:1 co-crystal, indicating that the system for
373 the 1:1 co-crystal is more disordered than the 2:1 co-crystals.
374 Therefore, 1:1 co-crystals in the solution state are less stable
375 than that of the 2:1 co-crystals. This further substantiates the
376 role of solvent sensitization on the outcome of co-crystal
377 formation.

378 The determination of the solubility curves was an important
379 method to differentiate and identify the polymorphic aspect of
380 this system. From the synthesis perspective of co-crystals for
381 this system, opting for water, ethanol, and mixed solvent
382 impacted the formation of pure 1:1 and 2:1 co-crystals, or a
383 mixture from both depending on the solvent composition.
384 These findings clearly support the view that the choice of mixed

solvent composition influences the step cooling crystallization 385
process significantly, and undertaking ternary phase diagram at 386
two temperatures which define initial and final point on step 387
cooling profile reveals the complex crystallization behavior of 388
1:1 or 2:1 co-crystal systems. 389

For the key crystallization parameters, solubility, induction 390
time, and under cooling, the impact of solvent composition has 391
been demonstrated to go beyond composition of BZ:INA 1:1 392
and 2:1 obtained but also impacts on the induction time for the 393
crystallization to occur. For instance when the solvent was 394
water, a notable induction time was seen; however, there was a 395
significant decrease in undercooling at 30% ethanol, with the 396
associated observation that the temperature of crystallization 397
was lower in water than ethanol, but of a similar magnitude 398
irrespective of solvent composition. Critically, such outcomes 399
do suggest these patterns with crystallization parameters do 400
trend with the picture of mixed modes of association and 401
solvation noted from the solubility screen. 402

To conclude, this contribution reveals the complexity of co- 403
crystal formation, for systems with 1:1 and 2:1 co-crystals, and 404
the way in which solvent composition, along with ternary phase 405
diagrams and solubility studies when combined as presented, 406
supports the rational design of the co-crystals crystallization. 407
Future work will be focused on the solution speciation and the 408
impact such speciation has upon the nucleation process for this 409
type of co-crystal system. 410

■ ASSOCIATED CONTENT

Supporting Information

The Supporting Information is available free of charge on the 413
ACS Publications website at DOI: 10.1021/acs.cgd.5b00908. 414

Van't Hoff equation; the log–linear model of Yalkowsky; 415
the Jouyban–Acree model; phase diagram experimental 416
(PDF) 417

■ AUTHOR INFORMATION

Corresponding Author

*E-mail: tmunshi@lincoln.ac.uk. 420

Notes

The authors declare no competing financial interest. 422

■ ACKNOWLEDGMENTS

This work was supported by Pfizer. 424

■ REFERENCES

- (1) ter Horst, J. H.; Deij, M. A.; Cains, P. W. *Cryst. Growth Des.* **2009**, 9, 1531. 426
- (2) Pudipeddi, M.; Serajuddin, T. M. *J. Pharm. Sci.* **2005**, 94, 929. 427
- (3) Blagden, N.; Davey, R. J. *Cryst. Growth Des.* **2003**, 3, 873. 429
- (4) Blagden, N.; Berry, D. J.; Parkin, A.; Javed, H.; Ibrahim, A.; Gavan, P. T.; De Matos, L. L.; Seaton, C. C. *New J. Chem.* **2008**, 32, 1659. 430
- (5) Seaton, C. C.; Parkin, A.; Wilson, C. C.; Blagden, N. *Cryst. Growth Des.* **2009**, 9, 47. 432
- (6) Chiarella, R. A.; Davey, R. J.; Peterson, M. L. *Cryst. Growth Des.* **2007**, 7, 1223–1226. 433
- (7) Jouyban, A.; Chew, N.; Chan, H.; Sabour, M.; Acree, W. E., Jr. *Chem. Pharm. Bull.* **2005**, 53, 634. 434
- (8) Soltanpour, S.; Acree, J. *Biomed. Int.* **2010**, 1, 9. 436
- (9) Acree, J. *J. Pharm. Pharmaceut. Sci.* **2008**, 11, 32. 437
- (10) Jouyban, A.; Panahi-Azar, V.; Khonsari, F. *J. Mol. Liq.* **2011**, 160, 14. 438
- (11) Jouyban, A.; Acree, W. *J. Mol. Liq.* **2008**, 142, 158. 439

- 444 (12) Jouyban, A. J. *Pharm. Sci.* **2008**, *11*, 32.
- 445 (13) Acree, W. E. *Thermochim. Acta* **1992**, *198*, 71.
- 446 (14) Boyd, S.; Chadwick, K.; Back, K.; Davey, R. j.; Seaton, C. C. J.
447 *Pharm. Sci.* **2010**, *99*, 3779.
- 448 (15) Prosim Ternary Phase Diagram software (<http://www.prosim.net/en/resources/download.html>).
- 449
- 450 (16) Ulrich, J.; Jones, M. *Chem. Eng. Res. Des.* **2004**, *82*, 1567.
- 451 (17) Huppert, H. E.; Sparks, R. S. J.; Wilson, J. R.; Hallworth, M. A.
452 *Earth Planetary Sci. Lett.*; Elsevier Science Publishers B.V.:
453 Amsterdam1986; pp 319–328.